Steady Nonlinear Response of a Barotropic Quasi-unidimensional Model to Complex Topography

R. BENZI,* S. IARLORI,* G. LIPPOLIS† AND A. SUTERA‡

*IBM ECSEC, Rome, Italy
†University of Genoa, Italy
‡St. Joseph College, West Hartford, Connecticut and Yale University, New Haven, Connecticut

(Manuscript received 7 January 1987, in final form 17 March 1988)

ABSTRACT

The response of a simple quasi-unidimensional barotropic model is studied. Wave–wave interaction, and bending the linear resonant response to the topographic forcing allows multiple equilibria if the zonal mean flow is assigned. The stationary solutions corresponding to the equilibria are compared with the observations.

1. Introduction

Recently it has been shown that the planetary-scale, Northern Hemisphere, winter eddy-field shows a bimodal probability density distribution (PDD), while the parameters characterizing the zonal-mean flow (speed, horizontal and vertical shear) show an unimodal PDD (see Sutera 1986; Hansen and Sutera 1986, 1987). If these observational results have to be interpreted in the context of a multiple-equilibrium theory of low-frequency variability such as Charney and DeVore (1979; hereafter CDV), some modifications to the theory are required. In fact, as discussed in Benzi et al. (1984) this theory requires bimodal PDDs for both eddy-field and zonal-mean flows. In eliminating this inconsistency, Benzi et al. (1986a; hereafter BMSS) showed that in a barotropic model it is necessary to fold the linear resonance response of the eddy-field to topographic forcing and to maintain a zonal-mean flow which is independent of the wave-field amplitude. In fact, for a preassigned zonal flow, the folding will guarantee multiple solutions of the equations for the perturbation field. Finally, Benzi et al. (1986b; hereafter BSS) showed that in a simple baroclinic model it was possible to remove the constraint of a fixed zonal-mean flow, thus partially restoring consistency between observational and theoretical results.

However, other inconsistencies arise. In fact, because of the linear nature of wave-field response to the topographic forcing in the CDV theory, the mere existence of the multiple equilibria depends on the existence of a resonant wave field. It has been argued that the atmospheric conditions for such a response are rarely met because the horizontal structure of the zonal-mean flow produces absorption of linear Rossby waves at the southern boundaries, rather than the reflection required by a resonance theory. (See Held 1983 for a review.) Moreover, if the CDV mechanism were responsible for the observed bimodality, then the two equilibrium circulations should show 180° phase reversal in going from one to the other state. Finally, if the equilibria of CDV have to be interpreted as the alternation of blocking and zonal circulation, the theory would have difficulties in accounting for the local nature of the balances which seem to preside in the blocking state.

In this paper we analyze these points in the context of a simple orographically forced nondivergent barotropic but nonlinear model. We will show that the inclusion of nonlinearity is sufficient to remove the above mentioned limitations.

2. A nonlinear model of multiple equilibria

In this section we describe the role of the topography in a simple nonlinear model of topographically forced stationary waves. As in CDV we consider the barotropic nondivergent vorticity equation in a β-channel,

$$\partial_t \Delta\psi + \mathcal{J}\left(\psi, \Delta\psi + \beta y + f_0 \frac{h}{H}\right) = -\nu\Delta\psi. \quad (1)$$

In this equation, $\mathcal{J}$, is the Jacobian operator, $f_0 = 2\Omega \sin\varphi_0$, $\beta = 2\Omega \cos\varphi_0/a$, Ω is the angular speed of the earth's rotation, a the radius of the earth, φ_0 a central latitude, H the equivalent depth of the atmosphere and h the topographic elevation, ν is the Ekman number. Here the x and y axes point eastward and northward, respectively. Choosing typical midlatitude values, we scale all our variables in the following way:

Corresponding author address: Dr. Alfonso Sutera, Dept. of Geology and Geophysics, Yale University, P.O. Box 6666, New Haven, CT 06511.

$$y = \frac{y}{L} \tag{2a}$$

$$x = \frac{x}{L} \tag{2b}$$

$$\psi = \frac{\psi}{U_0 L} \tag{2c}$$

$$h = \frac{h f_0 L}{H U_0} \tag{2d}$$

$$\beta = \beta \frac{L^2}{U_0} \tag{2e}$$

$$t = t \frac{U_0}{L} \tag{2f}$$

where L equals 1000 km, $f_0 = 10^{-4}$ s^{-1}, $U_0 = 10$ m s^{-1}, and $H = 10$ km. Our scaling implies that a geopotential amplitude of 100 m corresponds to $\psi = 1$.

As in CDV, let us consider the following stream function:

$$\psi = -Uy + \varphi(x, y, t). \tag{3}$$

Here U is the average zonal flow where the average is taken over the channel, i.e., the angular momentum. The equation for φ can be easily obtained from (1):

$$\partial_t \Delta\varphi + \beta\partial_x\varphi + U\partial_x\Delta\varphi + U\partial_x h + \mathcal{J}(\varphi, \Delta\varphi) + \mathcal{J}(\varphi, h) = -\nu\Delta\varphi + F. \tag{4}$$

As described in BMSS, in principle we should derive also an equation for U. In the absence of any baroclinic structure, the time evolution of U is controlled by the form-drag of the eddy fields and the friction. From BMSS, we know that by considering (4) coupled to the form-drag equation, we would get results inconsistent with the observations. (See also Tung and Rosenthal 1985.) Namely, the zonal wind would show a bimodal distribution with the modes unrealistically separated (by about 20–30 m s^{-1}). This problem can be avoided by considering a baroclinic atmosphere as shown in BSS. As reported there, in a baroclinic atmosphere the amplitude of the wave in the lowest layer can be taken as small as is wished, thus reducing the form-drag to a negligible effect. This is not possible in a barotropic model. With this in mind, despite the lack of mathematical rigor, we must neglect the form-drag equation if our purpose is to fit the statistical properties of the eddies' observed circulations by a barotropic model. Analogously, we neglect the equations for the other properties of the zonal mean wind (i.e., latitudinal shear) by requiring that φ has zero zonal mean.

As discussed in the Introduction, we want to introduce nonlinearity in the CDV model via wave–wave interaction. It might be argued that, in a model in which the zonal mean flow is independent of latitude, any inviscid, linear, topographically forced solution is also a solution of the full nonlinear problem. But it can be shown that no linear combination of linear topographically forced solutions is a solution of the full nonlinear problem. Hence we will consider solutions that allow wave–wave interaction by assuming

$$\psi = -Uy + \sum_n A_n(x, t) g_n(y), \quad n = 1 \cdots N \tag{5a}$$

$$h(x, y) = \sum_n g_n(y) h_n(x). \tag{5b}$$

It is obvious that the choice of equal latitudinal structure for the eddy-field and the topography implies that the eddy-field is projected on the latitudinal structure of the topography and neglects all the behavior which is projected onto the orthogonal subspace. It remains to be demonstrated that this is a good approximation. Furthermore, because of the nonlinearity of our equation, we have to artificially truncate the previous expression. Here we consider the case $n = 1$.

To illustrate the role of the topography in our model, we consider the inviscid case. In this case, a choice of g_1, which allows for wave–wave interaction, is

$$g_1(y) = \sin(\pi y/D) + \epsilon \sin(2\pi y/D), \quad 0 \leq y \leq D \tag{6}$$

where D is the width of the channel in dimensionless units (i.e., $D \to D/L$). For simplicity, we shall study the inviscid case. Thus, the stationary solutions of Eq. (4) projected on g_1 are given by

$$U(A_{xxx} + \alpha A_x) + \beta A_x - 3\delta A A_x + U h_x = 0 \tag{7}$$

where the subscript has been dropped and

$$\alpha \equiv \frac{\frac{1}{D}\int_0^D g g_{yy} dy}{\frac{1}{D}\int_0^D g^2 dy} = -\pi^2 \frac{(1 + 4\epsilon^2)}{D^2(1 + \epsilon^2)} \tag{8a}$$

$$\delta \equiv \frac{\frac{1}{D}\int_0^D g g_y g_{yy} dy}{\frac{1}{D}\int_0^D g^2 dy} = -\pi^3 \frac{3}{2} \frac{\epsilon}{D^3(1 + \epsilon^2)}. \tag{8b}$$

Let us assume that the topography has a single Fourier component in the zonal direction; i.e., $h(x) = h_0 e^{ikx} + h_0 e^{-ikx}$. Let us consider $A(x)$ given by

$$A(x) = A_1 e^{ikx} + A_2 e^{2ikx} + (*). \tag{9}$$

In the inviscid case, we can assume $A_1 = A_1^*$, and $A_2 = A_2^*$. We can easily obtain the equations for A_1 and A_2:

$$[\beta - (k^2 - \alpha)U]A_1 - 3\delta A_1 A_2 + Uh = 0 \tag{10a}$$

$$[\beta - (4k^2 - \alpha)U]A_2 - \frac{3}{2}\delta A_1^2 = 0. \tag{10b}$$

It is interesting to consider the solutions of (10a, b)

when h is small. For this purpose, let us assume $h = \hbar h'$ where $\hbar$ is a small parameter. Expanding A_1 and A_2 in powers of $\hbar$,

$$A_{i,j} = A_{i,j}^{(0)} + \hbar A_{i,j}^{(1)} + \cdots, \qquad i = 1, 2, \quad j = 1, 2, 3. \quad (11)$$

At the zero order we get

$$A_{1,1}^{(0)} = 0$$

$$A_{1,j}^{(0)} = \pm \frac{\sqrt{2[\beta - U(k^2 - \alpha)][\beta - U(4k^2 - \alpha)]}}{3\delta} \quad (12a)$$

$$A_{2,1}^{(0)} = 0 \quad A_{2,j}^{(0)} = \frac{\beta - U(k^2 - \alpha)}{3\delta} \quad j = 2, 3. \quad (12b)$$

Thus for $U > \beta(k^2 - \alpha)^{-1}$, two large amplitude solutions exist even in the limit of no topography as long as (5a) holds. By considering the next order, the three solutions are

$$A_{1,1} = A_1{}^{(0)} + \hbar A_1{}^{(0)} = \frac{Uh}{\beta - U(k^2 - \alpha)} + O(\hbar^2) \quad (13a)$$

$$A_{1,j} = A_{1,j}^{(0)} + \hbar A_{1,j}^{(0)}$$

$$A_{1,j} = \pm \frac{\sqrt{2[\beta - U(k^2 - \alpha)][\beta - U(4k^2 - \alpha)]}}{3\delta} + \frac{Uh}{2[\beta - U(k^2 - \alpha)]} + O(h^2), \quad j = 2, 3 \quad (13b)$$

$$A_{2,1} = O(\hbar^2) \quad (13c)$$

$$A_{2,j} = \pm \frac{Uh}{\sqrt{2[\beta - U(k^2 - \alpha)][\beta - U(4k^2 - \alpha)]}} + \frac{\beta - U(k^2 - \alpha)}{3\delta}, \quad j = 2, 3. \quad (13d)$$

Hence, it appears that in this model the role of the topography is merely to remove the zero solution at the resonant wave number, while introducing only a perturbatively small effect on the large amplitude solutions. This is a remarkable property which distinguishes our model not only from the CDV formulation of multiple equilibria but also from other studies of orographically forced waves. In fact, in contrast to studies such as Karoly and Hoskins (1981), Held (1983) and others, we have considered perturbations of a large amplitude wave regardless of the topographic forcing. This is a strong assumption that we maintain to be the foundation of our work. As a consequence, arguments depending on the propagation of small amplitude Rossby waves generated by the main orographic forcing do not apply directly to our work since our finite amplitude wave exists regardless of the structure of the zonal wind. Moreover, because the large amplitude solution is assumed to be weakly dependent on the topography, in a baroclinic model its existence would be also weakly dependent on the form-drag (see BSS) equation. Thus, there emerges a different picture from that presented in previous studies (see, e.g., Reinhold and Pierrehumbert 1982; BMSS, and BSS).

3. The problem of the phase in multiple-equilibrium theories

As discussed in the Introduction, CDV theory produces two equilibria which have a 180° phase difference. If we wish to interpret CDV equilibria as analogous to the bimodality detected in the data, this property should be found in the observations. In order to establish this link in Fig. 1a, b, we show the composite zonal profile of the latitudinally averaged geopotential 500-mb height (channel width 20° to 80°N) for each of the two modes (small and large amplitudes, respectively) determined in Sutera (1986, where the 500-mb composite charts are shown). The two profiles have been averaged over the four winters analyzed there.

By inspection of these two figures, it appears that the two modes differ mainly by their amplitude rather than the relative position of the ridges and troughs. Now the question arises as to whether a linear model can accommodate this feature. Of course, if the profiles of Fig. 1a, b were the response to the Northern Hemisphere topography, CDV, having only one zonal Fourier component of the topography, could not replicate this feature (and, in this instance, neither could the model of the previous section). In order to make the comparison more fair, we extended, as done by Charney et al. (1981; hereafter CSM), the zonal resolution of the topography. For this purpose, we project (4) into $g_1(y)$ and truncate at $n = 1$. Multiplying by $g_1(y)$ and integrating over y with the condition that $\{g_1{}^2\} = 1$, ($\{\cdots\} = \int \cdots dy$), we finally get

$$\partial_t(A_{xx} + \alpha A) + U(A_{xxx} + \alpha A_x) + \beta A_x - 3\delta A A_x + Uh_x = -\nu(A_{xx} + \alpha A) \quad (14)$$

where the coefficients are

$$\alpha \equiv -\{g_y{}^2\} \quad (15a)$$

$$\delta \equiv \{g g_y g_{yy}\}. \quad (15b)$$

where the subscript "1" has been dropped and terms proportional to $\gamma = \{ggg_y\}$ have been discarded because, in a closed channel, $\gamma = 0$.

The previous equations can be solved if we specify $h(x)$. Hereafter, $h(x)$ is as in CSM. Thus (14) differs from a CDV theory by essentially the nonlinear term $\delta A A_x$. To study the stationary solutions of (14), we have used the pseudoarclength continuation method due to Keller (1978), and recently applied by Legras and Ghil (1983), for purposes similar to ours. We refer to these papers for technical details.

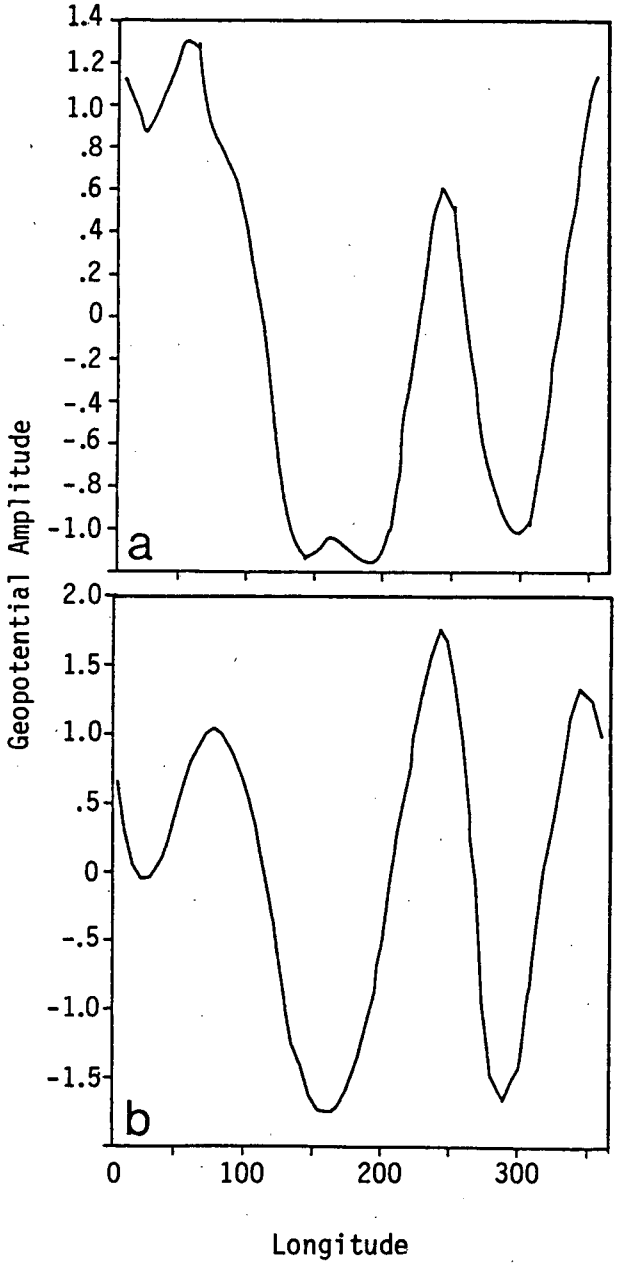

FIG. 1. (a) The average structure of a persistent anomaly corresponding to a blocked state. It has been obtained by using the bimodal indicator (Sutera 1986) and ECMWF data. (b) As in panel a, except for a "zonal state".

To compute the stationary solutions, we have followed the branch of solutions which cross the point at $U_0 = 0$, $A = 0$. Furthermore, we chose $\alpha = -0.53$ which corresponds to a channel width of 5000 km. All these values were maintained for all the computations.

We calculated the stationary solutions of (14) for $N = 128$ grid points and $\nu = 0.1$, which means a dissipation time of about 10 days (hereafter fixed). The algorithm has a performance of about 0.03 seconds for each stationary solution on the IBM3090/200VF.

First of all, we investigated the linear behavior of our system. We note that in the linear case ($\delta = 0$), $A(U)$ has the resonant peaks at

$$U = \beta/(K_0^2 - \alpha) \tag{16}$$

where K_0 is the zonal wavenumber. The maximum of the amplitude, A, is plotted against U in Fig. 2. It exhibits a clearly resonant structure, very close to that of the CSM model (CSM Fig. 2). The wavenumber-2 resonance is dominant for a value of the wind $U = 15$ m s^{-1}, and the wavenumber-3 ($U = 11$ m s^{-1}), -4 and -5 resonances are also noticeable. The wavenumber-2 peak is dominant because the topography has the maximum value of amplitude at this wavenumber. Figures 3a, b show the structure of equilibrium states for the subresonant and superresonant wavenumbers-2 as a function of x. There is good agreement between CSM and our model (for $\delta = 0$). As in CDV theories, the two equilibria show a remarkable phase reversal. It appears then that these theories are greatly in disagreement with respect to the observations. Next we will show that the inclusion of nonlinearity ($\delta \neq 0$) removes this disagreement.

In the nonlinear case, the stationary solutions were numerically computed employing the same values of parameters as in the linear case, but with $\delta = -0.5$. Figure 4 shows the result of this computation. First, we note that multiple solutions occur for superresonant values of U. This result is at variance with those of other investigators, namely Tung and Rosenthal (1985), Rambaldi and Mo (1984), and BMSS, where multiple solutions at fixed value U are found for subresonant values of U. In all these cases the bending was caused by interaction between the wave fields and

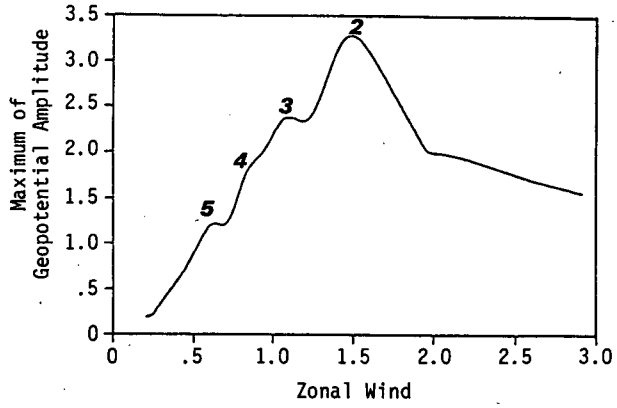

FIG. 2. Maximum of the geopotential amplitude A computed as a function of the zonal mean wind for the linear model ($\delta = 0$) unidimensional Eq. (15). The amplitude is expressed in hundred of meters and the zonal wind in m s^{-1}; $\alpha = -0.53$, $\nu = 0.1$, and $N = 128$ grid points. The integers at the peaks indicate the resonant topographic wavenumbers.

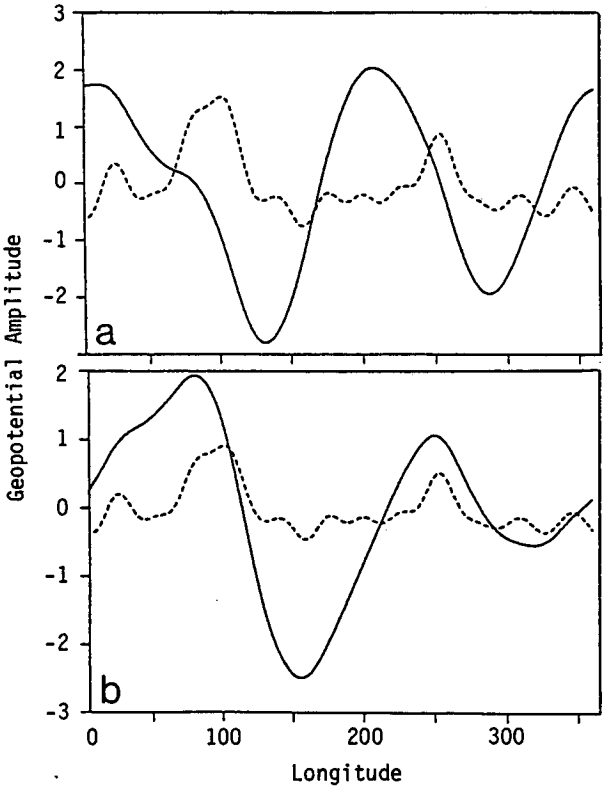

FIG. 3. (a) Subresonant wavenumber-2 linear solution as a function of longitude, for a value of the wind $U = 13$ m s^{-1}. This solution was computed from the linear stationary version of Eq. (15). The dashed lines represent the CSM topography. (b) Numerical super-resonant wavenumber-2 linear solution of Eq. (15) and CSM topography (dashed lines) against the longitude, with a value of the wind $U = 17$ m s^{-1}.

the latitudinal shear of the zonal mean flow, although in BMSS this effect was masked in the multiple-scale analysis of (14). In fact, in BSS at the first order in the perturbation scheme, the wave acquired a constant value independent of x consistent either with an infinite zonal channel or with a latitudinal shear in a zonally periodic channel. Here, as we have said, we consider a periodic channel with zero zonal mean perturbation field. There are implications associated with these choices—some of relevant physical importance—which are under current study.

We also note that for fixed value of the wind, the two extreme (in amplitude) states are always stable, while the intermediate one is unstable. The stability properties were verified with a time integration of (14) and we believe that they are preserved in absence of other instability, and also in a baroclinic model.

In Figs. 5a–c, we show the three solutions for

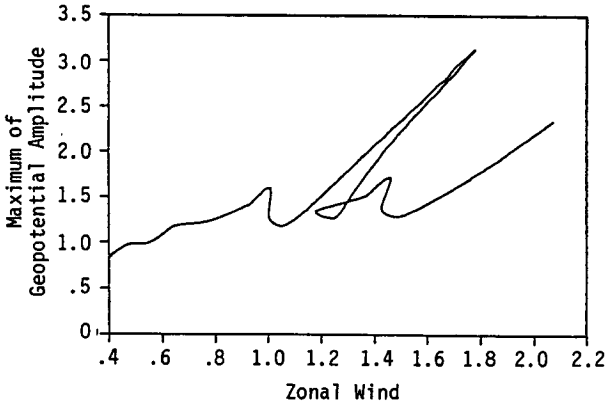

FIG. 4. The nonlinear resonance of the amplitude A (hundred of meters) against the zonal wind U (m s^{-1}), computed from the nonlinear Eq. (15). In this computation $\alpha = -0.53$, $v = 0.1$, $\delta = -0.5$, and $N = 128$.

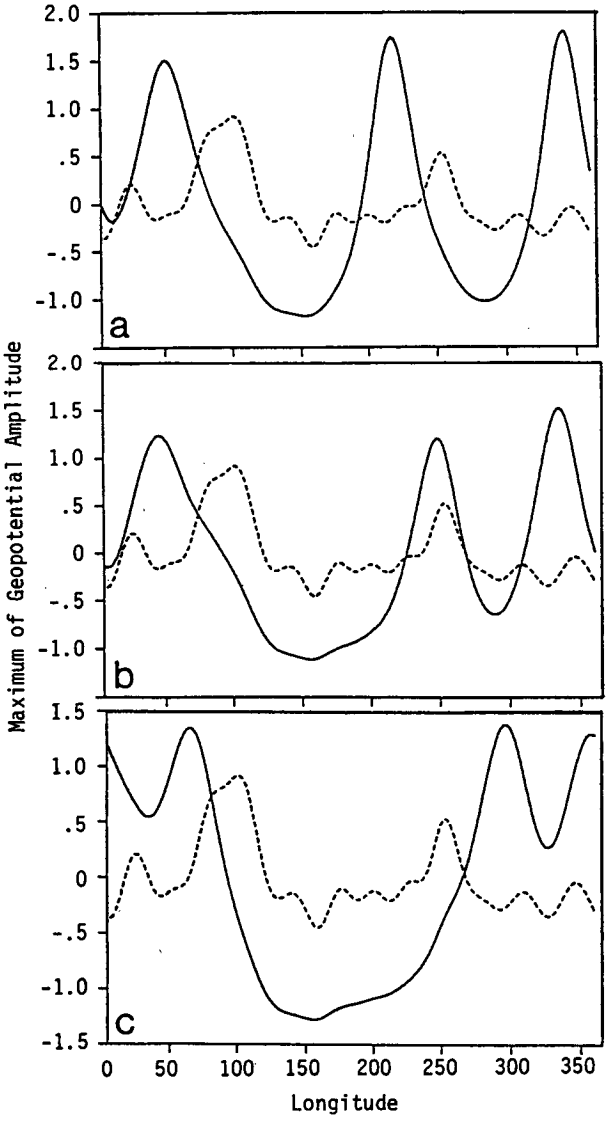

FIG. 5. (a) Subresonant wavenumber solution for the value of zonal wind $U = 13.5$ m s^{-1} against longitude, with the topography (dashed line); this solution corresponds to the nonlinear resonance structure, Fig. 4. (b) As in Fig. 5a, but for the intermediate state. (c) As in Fig. 5a, but for the zonal state.

$U \sim 13.5$ m s^{-1}, plotted with the topography as a function of longitude. Figure 5a shows the solution in the subresonant branch which corresponds to the upper portion of the curve.

Here, the wave anticipates the mountain, with a small negative shift of phase with respect to the mountain ridge. The peak before the Rocky Mountains appears localized and the whole configuration of the solution looks very much like the observed large amplitude state of Fig. 1a.

Figures 5b–c show the numerical solutions corresponding to the (unstable) intermediate branch and to the small amplitude solution, respectively. Major differences are evident between the small amplitude state of Fig. 5c and the observed composite result for the mode 1 state shown in Fig. 1b. In particular, in Fig. 5c the ridge near the Rockies is shifted eastward compared to Fig. 1b, and the trough in the Atlantic region is also too small. One possible explanation is that in our solution a wavenumber-1 pattern is dominant. This unrealistic response is probably due to the barotropic nature of our model. In a baroclinic case, the small amplitude state would be dominated by ordinary baroclinic activity and the full planetary-scale fields would be depleted. Nonetheless, we point out the small phase changes between these two solutions, in closer agreement with observations.

It is interesting to notice that the main difference between the small and large amplitude state of our model consist of an amplification of a wavenumber-3 pattern which agrees also with observations. Moreover, the large amplitude solution shows localized ridging with an amplitude of about 100 to 200 m, a feature shared by the observed profiles.

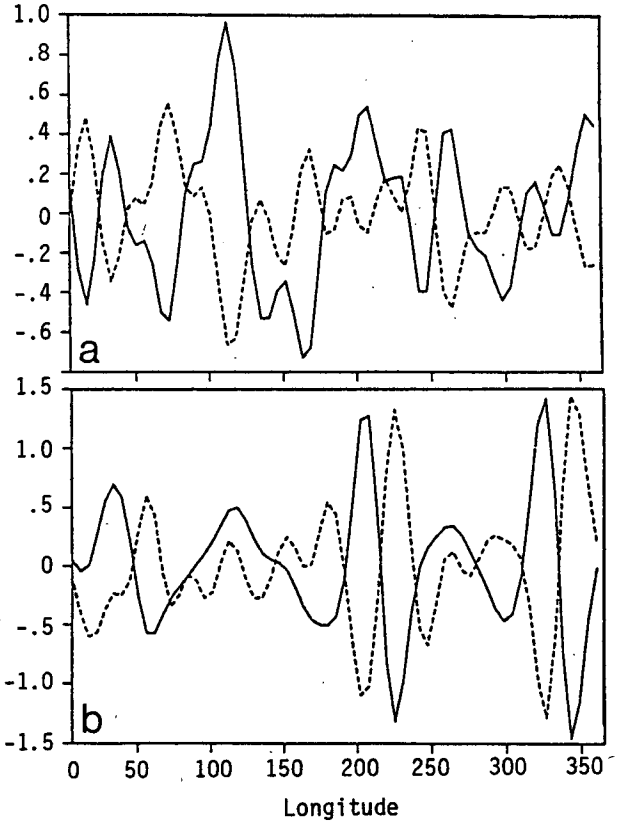

FIG. 6. (a) Plot of Uh_x (dashed line) and the dispersive part of Eq. (15), in the linear case, as a function of longitude. (b) Plot of δAA_x (dashed line) and the dispersive part of Eq. (15), in the nonlinear case, as a function of longitude.

4. The question of local versus global solution

Despite the global nature of the solutions of the nonlinear model, in the previous section we anticipated that the equilibria identified previously differ because of local amplification of portions of the profiles. To clarify this point more quantitatively, we analyzed the contributions of each term in the equation. Figure 6a shows the dispersive terms $\beta A_x + U(A_{xxx} + \beta A_x)$ and the orographic forcing Uh_x versus longitude for the linear case (Fig. 3a). A balance between the forcing term due to the orography and the dispersive part of the equation is evident. This is because the topography directly controls the amplitude of the solution. In Fig. 6b we plot the same dispersive term and the nonlinear term δAA_x for the solution shown in Fig. 5a. This time the nonlinear term balances the dispersive part of the equation; this is a feature (Malguzzi and Malanotte Rizzoli 1985) of the Kortgen-Devries equation, suggesting a solitonic behavior for our solution. In this case, wave–wave interaction affects the solution more than orography forcing and dissipation—a desirable feature for a baroclinic model of multiple equilibria such as the one discussed in BSS.

Finally, we remark that this result holds for a wide-range of δ as long as bending occurs.

5. Conclusion

In this paper it has been shown that including wave self-interaction in a CDV theory of multiple equilibria can eliminate some major inconsistencies between the theory of low-frequency variability and observations. In fact, it has been shown that no preassigned zonal-mean flow is necessary to obtain large amplitude solutions. Moreover, the small phase change shown by the observations between the two weather regimes identified by Sutera (1986) can be accounted for by the bending of the resonance. Finally, we showed how the nonlinear model can capture the local nature of the amplification of the underlying common wave pattern of the two regimes detected in the observations.

Acknowledgments. We are grateful to Drs. I. Held, and M. Mak, and an anonymous reviewer for constructive criticism which have helped to focus this work.

One of us (A. Sutera) acknowledges the support under NSF Grant ATM-86112226 at St. Joseph College.

REFERENCES

Benzi, R., A. R. Hansen and A. Sutera, 1984: On stochastic perturbation of simple blocking models. *Quart. J. Roy. Meteor. Soc.*, **110,** 393–409.

——, P. Malguzzi, A. Speranza and A. Sutera, 1986a: The statistical properties of general atmospheric circulation: Observational evidence and a minimal theory of bimodality. *Quart. J. Roy. Meteor. Soc.*, **112,** 661–674.

——, A. Speranza and A. Sutera, 1986b: A minimal baroclinic model for the statistical properties of low frequency variability. *J. Atmos. Sci.*, **43,** 2962–2967.

Charney, J. G., and J. G. DeVore, 1979: Multiple flow equilibria in the atmosphere and blocking. *J. Atmos. Sci.*, **36,** 1205–1216.

——, J. Shukla and K. C. Mo, 1981: Comparison of a barotropic blocking theory with observation. *J. Atmos. Sci.*, **38,** 762–779.

Hansen, A. R., and A. Sutera, 1986: On the probability density distribution of the planetary-scale atmospheric wave amplitude. *J. Atmos. Sci.*, **43,** 3250–3265.

——, and ——, 1987: The probability density distribution of the speed, horizontal and vertical shear of the zonal-mean flow. *J. Atmos. Sci.*, **44,** 1525–1533.

Held, I. M., 1983: The theory of stationary eddies. *Large Scale Dynamical Processes in the Atmosphere,* B. J. Hoskins and R. P. Pierce, Eds., Academic Press.

Karoly, D. J., and B. J. Hoskins, 1982: Three dimensional propagation of planetary waves. *J. Meteor. Soc., Jpn.*, **60,** 109–123.

Keller, H. B., 1978: Global homotopies and Newton Methods. *Nonlinear Analysis,* C. de Boor and G. H. Golub, Eds., Academic Press, 73–94.

Legras, B., and M. Ghil, 1983: Local blocking and variations in atmospheric predictability. *Predictability of Fluid Motion,* American Institute of Physics, N. G. Holloway and B. J. West, Eds., American Inst. of Physics, 106 pp.

Malguzzi, P., and P. Malanotte Rizzoli, 1985: Coherent structures in a baroclinic atmosphere. Part II: A truncated modal approach. *J. Atmos. Sci.*, **42,** 2463–2477.

Rambaldi, S., and K. C. Mo, 1984: Forced stationary solutions in a barotropic channel: Multiple equilibria and theory of non-linear resonance. *J. Atmos. Sci.*, **42,** 3135–3146.

Reinhold, B. B., and R. T. Pierrehumbert, 1982: Dynamics of weather regimes: Quasi-stationary waves and blocking. *Mon. Wea. Rev.*, **110,** 1105–1145.

Sutera, A., 1986: Probabilistic distributions of ultra long planetary waves in winter circulations. *Large Scale Anomalies and Blocking,* R. Benzi, B. Saltzman and A. Wiin-Nielsen, Eds., Academic Press.

Tung, K. K., and A. Rosenthal, 1985: Theories of multiple equilibria. Part III: A critical reexamination. Part I: Barotropic models. *J. Atmos. Sci.*, **42,** 2804–2819.